

# Transition from molecular complex to quantum solvation in ${}^4\text{He}_N\text{OCS}$

F. Paesani<sup>1,2</sup>, A. Viel<sup>1\*</sup>, F. A. Gianturco<sup>2</sup>, and K. B. Whaley<sup>1</sup>

<sup>1</sup>Department of Chemistry and Kenneth S. Pitzer Center for Theoretical Chemistry, University of California, Berkeley, CA 94704

<sup>2</sup> Department of Chemistry and INFM, University of Rome "La Sapienza", Città Universitaria, 00185 Rome, Italy  
(July 18, 2002)

We present quantum calculations of the rotational energy levels and spectroscopic rotational constants of the linear OCS molecule in variable size clusters of  ${}^4\text{He}$ , using spectral evolution quantum Monte Carlo methods that allow excited states to be accessed without nodal constraints. The rotational constants of OCS are found to decrease monotonically from the gas phase value as the number of helium atoms increases to  $N = 6$ , after which the average constant increases to saturation at a value in excellent agreement with experimental measurements made on significantly larger clusters ( $N \geq 1000$ ). The minimum is shown to indicate a transition from a molecular complex to a quantum solvated molecule, with the former characterized by floppy but near rigid behavior, while the latter is characterized by non-zero permutation exchanges and a smaller extent of rigid coupling.

PACS Numbers: 36.40.-c, 05.30.Jp, 61.46.+w, 67.40.Yv

Helium droplets offer a unique opportunity to immerse molecules into a superfluid. Spectroscopic experiments on molecules embedded in these droplets have yielded an array of measurements that provide on the one hand access to elementary excitations of the finite quantum liquid, and on the other hand information about the novel solvation dynamics encountered in a superfluid [1]. The rotational dynamics of the linear OCS molecule has played a key role in these spectroscopic studies. When solvated by the bosonic  ${}^4\text{He}$  isotope at temperatures  $T \leq 0.5$  K, infra-red spectra of OCS show rotational fine structure that is consistent with a free rotation accompanied by an increased molecular moment of inertia, while no fine structure is observed when OCS is solvated by fermionic  ${}^3\text{He}$  clusters [2]. Quantum Monte Carlo (QMC) calculations have confirmed that a spectrum of free rotational states with modified moment of inertia will result from bosonic solvation [3]. Such free rotation is not just the result of solvation by a fluid interacting with weak van der Waals forces. It has been shown to be consistent with a negligible transfer of angular momentum from the molecule to relative motion of the solvating helium when the latter possesses Bose permutation symmetry [4,3]. In contrast, efficient coupling to single-particle excitations in the fermionic  ${}^3\text{He}$  droplets has been shown to considerably reduce the lifetime of the rotational excitations [4], accounting for the absence of rotational spectral transitions.

Calculations of excited states afforded by QMC yield not only a direct route to calculation of spectroscopic constants for molecules solvated in helium, but they also provide critical insight into the nature of these rotational excitations. They thereby allow detailed microscopic

analysis of the quantum coupling between a molecule and its helium environment. Direct calculations of rotational energy levels have been made within dynamical approximations such as the quasi-adiabatic rigid coupling approximation [5,3] and fixed node approximations [6,7]. However, in order to provide a complete understanding of the underlying quantum dynamics, it is necessary to use a theoretical approach that allows *exact* calculation of excited states, devoid of any dynamical or nodal approximations. This is possible with the projection operator imaginary time spectral evolution (POITSE) approach, a diffusion-Monte-Carlo-based methodology that has recently been applied to calculation of rotational excitations of the linear HCN molecule in helium clusters [7]. For HCN, a considerably lighter molecule than OCS, these results showed a complex coupling between molecular and helium degrees of freedom that was attributed to the high zero point energy of the He-HCN system. In contrast, for the heavier octahedral molecule  $\text{SF}_6$ , rotational constants derived from fixed node calculations employing the free molecule nodal surfaces showed excellent agreement with experimental measurements [6].

In this letter we investigate the rotational motion of the OCS molecule inside  ${}^4\text{He}$  clusters, with direct calculations of rotational energy levels by POITSE. Analysis of the results in terms of rigid coupling approximations and of permutation exchanges visible in related finite temperature calculations allow for the first time a clear transition from a *molecular complex* to a molecule *solvated by a quantum liquid* to be identified as a function of cluster size  $N$ . OCS is intermediate in mass between HCN and  $\text{SF}_6$ . Comparison of the rotational behavior of OCS

\*current address: Lehrstuhl für Theoretische Chemie, Technische Universität München, 85747 Garching, Germany

with that of HCN and of SF<sub>6</sub> provides key insights into the quantum coupling of the molecular rotational motion with the solvating helium degrees of freedom, as a function of both molecular mass and symmetry.

Our calculations employ the Projector Operator Imaginary Time Spectral Evolution (POITSE) method for calculation of excited states [8]. In this scheme, excited state energies are extracted from the two-sided inverse Laplace transform of an imaginary time correlation function  $\tilde{\kappa}(\tau)$  that is computed by combining a multi-dimensional Monte Carlo integration with Diffusion Monte Carlo sidewalks. The decay of the correlation  $\tilde{\kappa}(\tau)$  contains information about energy differences  $E_f - E_0$ , where  $E_0$  is the ground state energy and  $E_f$  an excited state energy level. The POITSE approach is ideal for calculation of excitations in many-particle systems when estimates of excitation functions that take the ground state to the desired excited states are available. A suitable correlation function is then

$$\tilde{\kappa}(\tau) = \frac{\langle \Psi_T | \hat{A} \exp[-(\hat{H} - E_0)\tau] \hat{A}^\dagger | \Psi_T \rangle}{\langle \Psi_T | \exp[-(\hat{H} - E_0)\tau] | \Psi_T \rangle}, \quad (1)$$

where  $\hat{A}$  is a local operator that projects from a trial function  $|\Psi_T\rangle$  approximating the ground state  $|\Psi_0\rangle$ . The resulting initial state  $\hat{A}^\dagger |\Psi_T\rangle$  is usually not an eigenfunction of  $\hat{H}$ , but time evolution under the action of the full Hamiltonian will ensure that all eigen components  $|\Psi_f\rangle$  that overlap with this state will contribute to the correlation function. Inverse Laplace transform of  $\tilde{\kappa}(\tau)$ , performed by the maximum entropy method as described in Ref. [8], results in the spectral function

$$\kappa(\omega) = \sum_f |\langle \Psi_T | \hat{A} | \Psi_f \rangle|^2 \delta(E_0 - E_f + \omega), \quad (2)$$

from which all excitation energies accessed by  $\hat{A}$  may be extracted as the peak locations. When  $|\Psi_T\rangle \equiv |\Psi_0\rangle$ , exact energies are obtained, while otherwise some trial function bias may exist [8].

Our approach to extract the rotational excitations of interest is to take a free molecular projector acting on the molecule-helium cluster ground state. Since the molecule-helium coupling is weak, this provides a good starting point for calculation of the imaginary time correlation function and subsequent spectral transformation. For the trial function  $\Psi_T$  we employ variationally optimized ground state functions of the usual generalized product form, namely containing pairwise correlations between all components of the cluster, *i.e.*, isotropic He-He and anisotropic He-OCS terms. The He-He correlations are those used in Ref. [9], while the He-OCS correlations take the form  $\chi(R, \theta; \{p_i\}) = \exp\{p_0 R^{p_1} + p_2[1 + p_3 \cos(\theta - p_4) \ln R] + p_5 R^2 \cos^2(\theta - p_4) e^{(p_6 - p_7 R)}\}$  where  $R, \theta$  are the Jacobi coordinates describing the location of the He atom relative to the linear OCS molecule [9].

We consider here projectors  $\hat{A}$  proportional to the molecular Wigner functions  $D_{mk}^j$  in a space-fixed frame. Zeros of  $D_{mk}^j$  constitute free molecule nodal surfaces for a symmetric top [11]. We focus here in particular on  $j = 1, m = k = 0$ , a linear rotor eigenfunction for which  $\hat{A} = \cos \beta$  is a function only of the second Euler angle of the molecule specifying the orientation of the molecular frame in the (arbitrary) space-fixed frame.  $\hat{A}$  accesses states in which the total angular momentum  $J$  is carried primarily by the OCS, *i.e.*, the molecular angular momentum  $j$  is a quasi-good quantum number and there is negligible angular momentum  $l$  in the relative helium motion ( $\mathbf{J} = \mathbf{j} + \mathbf{l}$ ). Our choice of  $D_{00}^1$  is motivated by analysis of the calculated rotational spectrum for the He-OCS complex ( $N = 1$ ) [10] which shows that this is the primary molecular function contributing to the  $J_{K_p, K_o} = 1_{01}$  rotational state of the complex. (We employ here the notation  $J, K_p, K_o$  for rotational states of an asymmetric rotor [11].)

We emphasize that the projector  $\hat{A}$  provides only an initial guess for the nodal structure of the excitations, and that these automatically adjust to their true values during the calculation. That these are indeed subtly different from the free nodal surfaces for OCS is evident from the fact that for  $N = 1$ , a 5-dimensional system where exact calculations are possible using *e.g.*, the BOUND program [12], fixed node calculations carried out with nodal constraints imposed by the Wigner function do not show good agreement with the exact calculations, overestimating the exact rotational excitation energy for OCS-He ( $0.307 \text{ cm}^{-1}$ ) by  $0.07 \pm 0.01 \text{ cm}^{-1}$ , *i.e.*, 22(3)%. In contrast, POITSE gives the exact energy to within a statistical error of 0.7%, *i.e.*,  $0.309 \pm 0.002 \text{ cm}^{-1}$ . This behavior contrasts with the high accuracy of the free molecule fixed node approximation found for the heavier SF<sub>6</sub>-He complex. [6]

The total molecule-cluster interaction potential is the sum of all pairwise contributions (He-He and OCS-He). We have employed two recent He-OCS potentials [10,13] and find equivalent results with these. Unless otherwise stated, all calculations reported here are made with the *ab initio* HHSDS He-OCS potential energy surface [10] and the HFD-B He-He potential of Ref. [14]. The imaginary time evolution is performed with the rotational importance-sampled rigid body Diffusion Monte Carlo algorithm of Ref. [15]. Initial ensembles of 1000 walkers distributed according to  $|\Psi_T|^2$  were propagated for 30,000 steps of  $\Delta\tau = 50$  a.u. using the mixed branching/weight algorithm of Ref. [16]. Typically 1000-2000 independent decays were required to produce a converged spectrum  $\kappa(\omega)$ , with the largest size ( $N = 20$ ) requiring the most decays. Statistical error bars in the excitation energies were estimated using a Gaussian approximation, according to the procedure described in Ref. [17].

POITSE calculations with the Wigner projector  $\hat{A}$

consistently produced only one peak in the  $\kappa(\omega)$  spectrum, for all sizes  $N \leq 20$ . This clean single-valued behavior of the free molecule projector for OCS contrasts with the behavior seen earlier for the lighter HCN molecule, where the same projector leads to multiple excited states [7]. Single-valued free molecule projectors suggest that  $\hat{A}|\Psi_T\rangle$  is very similar to the true eigenstate. However, free or quasi-free rotations do not prohibit effective rigid coupling of some solvating helium density to the molecular rotation, leading to a renormalization of the molecular moment of inertia similar to that found in the microscopic two-fluid theory [3] and in perturbative analysis [4].

When interpreted with an asymmetric top Hamiltonian [11], the cluster rotational excited state energy derived from  $\hat{A}$ ,  $E(J_{K_p, K_o} = 101)$ , yields an effective rotational constant  $B_{avg}$ . When close to the limit of a symmetric top,  $B_{avg}$  is equal to either  $(B+C)/2$  (prolate top) or  $(A+B)/2$  (oblate top). Fig. 1 shows the main result of this paper, namely the behavior of  $B_{avg}$  obtained from the POITSE calculations, as a function of cluster size  $N$ . Corresponding experimental values of  $B$  for the free (gas phase) OCS molecule and for OCS in large helium droplets ( $N \geq 1000$ ) where the spectrum was fit to a linear rotor ( $B_{avg} \equiv B$ ) are shown from Ref. [18]. For the smallest clusters  $N = 1$  [13] and  $N = 2$  [19] we show the experimentally measured values of  $B_{avg}$ .

The POITSE results show a monotonic decrease of the excited state energy up to  $N = 6$ , followed by a small continuous increase to saturation at a value  $B_{avg} = 0.07(2)$   $\text{cm}^{-1}$  that is in excellent agreement with the experimentally measured value  $B = 0.0732(3)$   $\text{cm}^{-1}$  in large droplets [18]. Excellent agreement of  $B_{avg}$  with the corresponding experimental values  $B_{avg}$  for small clusters is also achieved for the two sizes  $N=1, 2$  for which this experimental data is available [13,19]. Thus the POITSE calculations are able to bridge the gap between small van der Waals clusters and large droplets, achieving high accuracy in both regimes. The overall behavior of  $B_{avg}$  for OCS shows some similarities with  $\text{SF}_6$  and with HCN, but also exhibits critical differences from these molecules. For the more symmetrical and heavier  $\text{SF}_6$  molecule the saturation value is also reached before the first solvation shell is completed ( $N \simeq 8$ ) but negligible overshoot is seen [6]. For the lighter HCN, also linear, a large overshoot is seen but the rotational constant does not reach saturation before completion of the first solvation shell [7].

A deeper understanding of the size dependent quantum coupling within these rotational excitations in the bosonic  ${}^4\text{He}$  cluster is provided by analysis in terms of both rigid coupling models and permutation exchange distributions. The triangle symbols in Fig. 1 show the values of  $B_{avg}$  obtained using the quasi-adiabatic rigid coupling approach [5,3] implemented with correlated sampling [20]. The POITSE results are very close

to the rigid coupling estimates for  $N \leq 6$ , with the latter lying consistently slightly lower than the corresponding POITSE values. Within a rigid coupling approximation, the complete  ${}^4\text{He}$  density is assumed to adiabatically follow the rotational motion of OCS. Therefore the systematically higher values of the POITSE results is a direct manifestation of only *partial* adiabatic following of the solvating helium density with OCS rotation. The quasi-adiabatic rigid coupling approach does incorporate all zero point motions. This results in the intersection at  $N = 4$  of the rigid coupling estimate of  $B_{avg}$  with the experimental  $B$  value in large droplets, in contrast to the crossing at  $N=6$  estimated in Ref. [18] from a classical binding model that neglects zero point energy. The actual crossing point is in remarkable agreement with the integral of the molecule-induced local non-superfluid density calculated by path integral methods in Ref. [3] ( $n_{ns} \sim 3.2$ ), and is thus consistent with the analysis made there of a reduced  $B$  deriving from rigid coupling to the local non-superfluid density in the first solvation shell. The quasi-adiabatic rigid coupling estimates fail at larger sizes, where they necessarily continue to decrease monotonically, reaching negligible values by  $N \sim 50$ . Table I shows the quasi-adiabatic rigid coupling results for all three rotational constants  $A, B$  and  $C$ , for selected cluster sizes. This indicates that the asymmetric top spectrum ( $A > B > C$ ) evolves into a prolate symmetric top spectrum ( $A > B = C$ ) by  $N = 10$ , the same size at which the POITSE  $B_{avg}$  reaches the asymptotic droplet value of  $B$  (Fig. 1). However, we expect that the transition between asymmetric and symmetric top may occur at a different cluster size for the exact calculations.

One of the most interesting features of the POITSE results seen in Fig. 1 is the turn-around of  $B_{avg}$  at relatively small  $N$ , and subsequent rise to saturation at the experimental large droplet value by  $N = 10$ . This behavior is related to the onset and nature of permutation exchanges between the  ${}^4\text{He}$  atoms. It can be quantitatively interpreted in terms of these exchanges [21] and of the structures previously analyzed in terms of the axial solvation locations in Ref. [20]. As shown there, while for  $N \leq 5$  the helium density is essentially localized in the global minimum of the He-OCS potential energy surface, as  $N$  increases beyond 5 the additional helium atoms solvate other regions along the molecule, covering the entire axial extent of the OCS molecule by  $N = 10$ . Path integral calculations show no permutation exchanges for  $N \leq 5$ , but as  $N$  increases above 5 and the helium density grows along the molecular axis, exchange permutations are seen, with components both along and around the molecular axis [21]. The lack of exchanges for  $N \leq 5$  is attributed to the difficulty of exchanging within a single tightly packed axial ring, and accounts for the near rigid behavior at these sizes. The permutation exchange path components along the molecular axis seen

for  $N \geq 6$  result in a lowering of the corresponding rigid body response for rotation about axes perpendicular to the molecule (*i.e.*, to a non-zero perpendicular superfluid response), causing in a rise in rotational constants  $B$  and  $C$  [22]. This effect continues as the solvation layer grows along the molecular axis and the lateral permutation exchange contributions increase, thereby accounting for the observed increase in the POITSE values over the range  $N = 6 - 10$  in Fig. 1. Note that  $N = 10$  is the first size at which the  ${}^4\text{He}$  density extends along the entire molecular axis [20], thereby allowing permutation exchanges of maximal extent within the first solvation shell, *i.e.*, from one end of the molecule to the other. We conclude that for OCS the range  $N = 6 - 10$  with its increase of  $B_{avg}$  to saturation from an overshoot at  $N = 6$  denotes a transition between a van der Waals (molecular) complex and a true quantum solvated molecule. The complex is 'near rigid', or 'floppy', in spectroscopic language, while the quantum solvated molecule is characterized by permutation exchanges between the helium atoms [3]. For large enough clusters, the latter leads to a microscopic local two-fluid description of co-existing superfluid and non-superfluid densities within the first solvation shell [23,3].

In conclusion, we have provided calculation of rotational constants for OCS-doped  ${}^4\text{He}$  clusters containing up to one complete solvation shell ( $N = 1 - 20$ ), by a direct method without imposing dynamical or nodal approximations. We find accurate agreement with experimental results at both extremes of small size  $N = 1, 2$ , and large droplets. These POITSE calculations allow for the first time the transition from a molecular complex to a quantum solvated molecule in superfluid  ${}^4\text{He}$  to be precisely identified, and interpreted in terms of the quantum structure and permutation exchange propensity of the local helium environment.

*Acknowledgements:* This work was supported by the NSF (CHE-9616615, CHE-0107541) and by the Italian Ministry for University and Research (MUIR). We thank NPACI and CASPUR for computation time at the San Diego Supercomputer Center and the University of Rome Computing Center, respectively.

TABLE I. Rotational constants (in  $\text{cm}^{-1}$ ) calculated by the quasi-adiabatic rigid coupling method with two different He-OCS potential energy surfaces, shown for clusters having  $N \leq 10$   ${}^4\text{He}$  atoms.  $A, B, C$ : from HHDSD potential [10].  $A', B', C'$ : from MP4 potential [13].

$N$	$A$	$A'$	$B$	$B'$	$C$	$C'$
1	0.457(2)	0.443(2)	0.175(2)	0.173(2)	0.123(2)	0.120(2)
2	0.208(2)	0.202(2)	0.128(2)	0.129(2)	0.092(1)	0.092(1)
4	0.101(2)	0.098(1)	0.074(1)	0.077(1)	0.062(1)	0.065(1)
6	0.067(1)	0.065(1)	0.051(1)	0.052(1)	0.044(1)	0.045(1)
7	0.057(1)	0.056(1)	0.045(1)	0.045(1)	0.038(1)	0.039(1)

- [1] See, e.g., J. P. Toennies, A. F. Vilesov and K. B. Whaley, *Phys. Today*, **54**, 31 (2001) and ref. therein.
- [2] S. Grebenev, J. P. Toennies, and A. F. Vilesov, *Science* **279**, 2083 (1998).
- [3] See Y. Kwon *et al.*, *J. Chem. Phys.* **113**, 6469 (2000) and ref. therein.
- [4] V. S. Babichenko and Y. Kagan, *Phys. Rev. Lett.* **83**, 3458 (1999).
- [5] M. Quack and M. A. Suhm, *J. Chem. Phys.* **95**, 28 (1991).
- [6] E. Lee, D. Farrelly, and K. B. Whaley, *Phys. Rev. Lett.* **83**, 3812 (1999).
- [7] A. Viel and K. B. Whaley, *J. Chem. Phys.* **115**, 10186 (2001).
- [8] D. Blume, M. Lewerenz, P. Niyaz, and K. B. Whaley, *Phys. Rev. E* **55**, 3664 (1997).
- [9] F. Paesani, F. A. Gianturco, and K. B. Whaley, *J. Chem. Phys.* **115**, 10225 (2001).
- [10] F. A. Gianturco and F. Paesani, *J. Chem. Phys.* **113**, 3011 (2000).
- [11] R. N. Zare, *Angular Momentum* (Wiley, New York, 1988).
- [12] Exact calculations made with BOUND, version 5, distributed by Collaborative Computational Project No. 6 of the Science and Engineering Research Council (U.K.).
- [13] K. Higgins and W. H. Klemperer, *J. Chem. Phys.* **110**, 1383 (1999).
- [14] R. A. Aziz, F. R. W. McCourt, and C. C. K. Wong, *Mol. Phys.* **61**, 1487 (1987).
- [15] A. Viel, M. V. Patel, P. Niyaz, and K. B. Whaley, *Comp. Phys. Com.* **145**, 24 (2002).
- [16] P. Huang, A. Viel, and K. B. Whaley, in *Recent Advances in Quantum Monte Carlo Methods, Part II* (Lester, Jr., W. A. and S. M. Rothstein and S. Tanaka, World Scientific, Singapore, 2002), Vol. 2, p. 111.
- [17] D. S. Sivia, *Data Analysis: a Bayesian Tutorial* (Oxford University Press, Oxford, 1996).
- [18] S. Grebenev *et al.*, *J. Chem. Phys.* **112**, 4485 (2000).
- [19] Y. Xu and W. Jager, *Chem. Phys. Letters* **350**, 417 (2001).
- [20] Values of the asymmetric top rotational constant  $B$  were reported for  $N \leq 10$  in F. Paesani, F. A. Gianturco, and K. B. Whaley, *Europhys. Lett.* **56**, 658 (2001).
- [21] Y. Kwon and K. B. Whaley, to be published.
- [22] Y. Kwon and K. B. Whaley, *Phys. Rev. Lett.* submitted (2002).
- [23] Y. Kwon and K. B. Whaley, *Phys. Rev. Lett.* **83**, 4108 (1999).

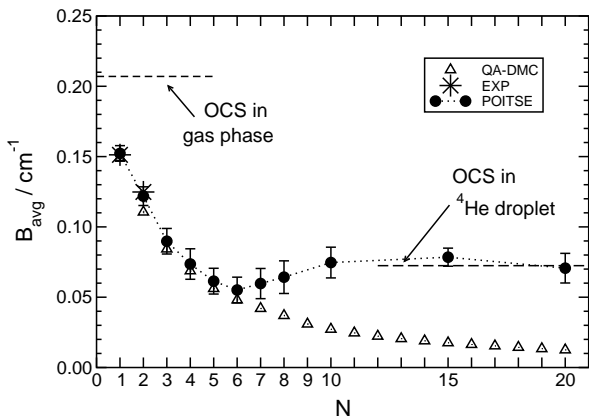


FIG. 1. Effective rotational constant  $B_{avg}$  for OCS in  ${}^4\text{He}_N$ , as a function of cluster size  $N$ . Circles show POITSE results obtained from cluster rotational state energies generated by projectors  $\hat{A} = \cos(\beta)$  (see text). Triangles show quasi-adiabatic rigid coupling estimates [20], asterisks correspond to the experimental values of  $B_{avg}$  for  $N=1,2$  [13,19]. The latter are seen to be coincident with the POITSE results (circles). Gas phase and experimental values in large  ${}^4\text{He}$  droplets are taken from Ref. [18].